

To be submitted for publication in the ApJ

## An Alignment Effect in FR I Radio Galaxies: U-band Polarimetry of the Abell 2597 Cluster Central Galaxy

Brian R. McNamara<sup>1</sup>

Harvard-Smithsonian Center for Astrophysics  
60 Garden St.  
Cambridge, MA 02138

Buell T. Jannuzi

National Optical Astronomy Observatories  
P.O. Box 26732  
Tucson, AZ 85726-6732

Craig L. Sarazin

Astronomy Department  
University of Virginia  
P.O. Box 3818  
Charlottesville, VA. 22903-0818

Richard Elston

University of Florida  
Department of Astronomy  
211 Space Sciences Bldg.  
Gainesville, FL 32611-2055

Michael Wise

MIT  
Center for Space Research  
MS 37-667  
Cambridge, MA. 02139-4307

arXiv:astro-ph/9810465v1 28 Oct 1998

---

<sup>1</sup>Visiting Astronomer, Kitt Peak National Observatory. KPNO is operated by AURA, Inc. under contract to the National Science Foundation.

## ABSTRACT

We have obtained U-band polarimetry of the spatially extended, blue optical continuum associated with the FR I radio source PKS 2322–122. PKS 2322–122 is located in the Abell 2597 cluster central galaxy. We find a three sigma upper limit to the degree of polarization of the optical continuum of less than 6%. The accuracy of the measurement is limited primarily by our ability to measure the amount of diluting galactic starlight. This limit is inconsistent with the blue continuum being primarily scattered light or synchrotron radiation. We can therefore exclude models which attribute the blue continuum to scattered light from an active nucleus that is hidden from direct view. Our result does not support the unification paradigm for BL Lac objects and FR I radio sources.

Essentially all of the data pertaining to the blue continuum along the radio source—the “blue lobes”—indicate that they are regions of recent star formation. The spatial coincidence between the blue lobes and disturbances in the radio source suggests that star formation may have been induced by an interaction between the radio source and the cool ( $< 10^4$  K), surrounding gas. This result, in addition to the results of a similar study of the A1795 cluster central galaxy, shows that under the appropriate conditions FR I radio sources may be capable of inducing significant episodes of star formation in elliptical galaxies.

We compare the restframe U-band polarized luminosities and 1.4 GHz radio powers of A2597 and A1795 to those for several high redshift radio galaxies exhibiting the alignment effect. We find that if the polarized luminosities of radio galaxies scale in proportion to their radio luminosities, we would not have detected a polarized signal in either A2597 or A1795. We suggest that the fundamental property distinguishing some powerful, high redshift radio galaxies exhibiting the alignment effect, and the lower-power, FR I radio galaxies in cooling flows that exhibit the blue lobe phenomenon, is the strength of the AGN. While both FR I and FR II radio sources seem to be capable of triggering star formation, FR I radio sources seem to be incapable of producing a large enough polarized luminosity to contribute significantly to the aligned continuum radiation.

*Subject headings:* BL Lacertae objects: general — cooling flows — galaxies: clusters: individual (A2597) galaxies: elliptical and lenticular, cD — polarization — radio continuum: galaxies — galaxies: active — galaxies: clusters: general — galaxies: jets — intergalactic medium — radiation mechanisms: non-thermal — scattering — techniques: polarimetric — ultraviolet: galaxies

## 1. Introduction

The well known tendency for the blue optical continuum in distant, luminous radio galaxies to be aligned with their radio sources represents a potentially important evolutionary phase of radio galaxies. The blue optical continuum associated with the Fanaroff-Riley class two (FR II) radio sources in powerful radio galaxies often extends several tens of kiloparsecs into their halos along the axis of the radio source. The extended radio and optical continuum is usually associated with bright nebular emission. This so-called “alignment effect” becomes increasingly prominent in powerful radio galaxies at redshifts  $z \gtrsim 0.6$ , but is rarely strong in radio galaxies at redshifts less than  $z = 0.1$  (see McCarthy 1993 for a review).

Distant, FR II radio sources are frequently bent and distorted in the vicinity of strong nebular emission. The nebular gas velocity fields are usually turbulent and shearing, with characteristic velocities of several hundreds of kilometers per second. Such properties seem to indicate that strong interactions (e.g. momentum exchange, photon heating and ionization) are occurring between the radio source and the nebular gas. Remarkably, processes associated with the radio source, which originates in a powerful nuclear engine, can affect the photometric properties of the host galaxy to large galactic distances.

Several emission mechanisms have been proposed to explain the extended, blue optical continuum including star formation, scattered light from an obliquely-directed active nucleus, synchrotron radiation, nebular continuum, and inverse Compton radiation (di Serego Alighieri et al. 1989; Fabian 1989; De Young 1989; Rees 1989; Begelman & Cioffi 1989; Daly 1990, 1992; Dickson et al. 1995). Although each of these emission mechanisms is interesting in its own right, collectively they imply essentially two important consequences for the evolution of radio galaxies. Star formation at the implied levels of several tens to over a thousand solar masses per year (e.g. 4C41.17, Dey et al. 1997) would have a significant impact on the development of the stellar composition and structure of the host galaxy. The remaining emission mechanisms in general imply the presence of a powerful central engine, a dense interstellar medium, and strong magnetic fields, but may be otherwise inconsequential to the development of the stellar composition and structure of the galaxy. However, the alignment effect cannot be reduced to a unique mechanism, as one or more of these emission mechanisms may contribute significantly to the effect in a particular galaxy and among galaxies.

It has been known for some time that central dominant cluster galaxies (CDGs) selected on the basis of high surface brightness X-ray emission tend to have unusually blue cores accompanied by bright, spatially extended nebular emission, and Fanaroff-Riley class 1 (FR I) radio sources (Baum 1992; Cardiel, Gorgas, & Aragon-Salamanca 1997; McNamara 1997). Furthermore, the bright, blue continuum in two objects (the A2597 and A1795 CDGs) lies along their radio sources in a manner similar to the high redshift, FR II radio galaxies, but on a smaller scale. Although these two objects share some of the alignment properties seen in FR IIs, they are noteworthy in several respects. They reside at the centers of bright, cluster-scale, thermal X-ray emission that has been interpreted as the signature of a large reservoir of cooling gas (i.e. a “cooling flow”). They harbor less-luminous, FR I radio sources whose 1.4 GHz radio powers are less than

$10^{26} \text{ W Hz}^{-1}$ , and their aligned blue continuum, or “blue lobes”, is preferentially associated with their radio lobes, rather than their radio jets. Finally, A2597 and A1795 are relatively nearby at redshifts of 0.082 and 0.064 respectively. A redshift or radio luminosity dependence on the degree and frequency of strong alignments would suggest an active evolutionary phase of radio galaxies that occurred at a special cosmic epoch or under special circumstances.

In order to explore the emission mechanism of the radio-aligned continua in the A2597 and A1795 CDGs, we have obtained U-band polarimetry of the blue continuum along their radio sources. Polarimetry can be used to discriminate between the two favored emission mechanisms: highly polarized scattered light from a hidden active nucleus (Sarazin & Wise 1993; Crawford & Fabian 1994; Murphy & Chernoff 1993; Sarazin et al. 1995) and the unpolarized light from star formation (MO93; De Young 1995). The scattering model was proposed in part because of its success in explaining the often highly polarized continuum in the distant FR II radio galaxies (di Serego Alighieri et al. 1989; Scarrott, Rolf & Tadhunter 1990; Jannuzi & Elston 1991; Tadhunter et al. 1992; di Serego Alighieri, Cimatti & Fosbury 1993; Antonucci 1993; Jannuzi 1994; Jannuzi et al. 1995; Dey et al. 1996; Cimatti et al. 1997), and in response to the paradigm that seeks to unify FR I radio sources and BL Lac objects (Urry and Padovani 1995). The scattering models are appealing in the cases of A2597 and A1795 because the dense and dusty environments associated with their cooling flows provides a suitable scattering medium, were the FR I radio sources indeed BL Lac objects seen at an oblique angle to the line of sight (Padovani & Urry 1990; Urry and Padovani 1995; Sarazin & Wise 1993; Murphy & Chernoff 1993). Were the blue lobes shown to be highly polarized with the electric vectors orthogonal to the radio axis, the result could be interpreted as a significant step toward verifying such a “unified scheme.”

We have addressed these issues using sensitive U-band polarimetric observations of the blue lobes. Although these galaxies are intrinsically faint at U, and the throughput of the telescope and polaroid filter at U are low, the U-band offers the largest contrast between the blue continuum and the red background population of the cD galaxy. The U-band is therefore most sensitive to the blue continuum and least prone to error when estimating the amount of presumably unpolarized background light that would dilute any polarized signal from the blue lobes. The background starlight limits the accuracy of the polarization measurements (§4.1). Therefore, minimizing the amount of dilution by starlight is critical to maximizing the sensitivity to low levels of polarized light. In addition, shorter wavelength observations are more useful for comparison to the high redshift FR II radio galaxies, where R and I-band observations correspond to rest wavelengths in the U-band.

In a study similar to that presented here for A2597, we found A1795’s aligned continuum, or blue lobes, to be unpolarized (McNamara et al. 1996a). In subsequent papers the lobes were shown to be resolved into what appear to be star clusters using images obtained with the Hubble Space Telescope (McNamara et al. 1996b; Pinkney et al. 1996), clearly demonstrating the emission mechanism for the lobes in A1795 to be a population of young stars. In this paper we present the results of a similar polarimetric study of the blue lobes in the A2597 CDG.

## 2. Observations

The images were obtained with the Mayall 4 meter telescope of the Kitt Peak National Observatory during the nights of 8, 9, and 10 November, 1996. We used the Tektronix  $2048 \times 2048$  pixel (scale= 0.47 arcsec/pixel) CCD detector mounted at the prime focus. The Q and U Stokes parameter images were constructed from a series of exposures obtained through a combination of a U-band filter attached to a copper sulfate blocking filter, and one of four Polaroid filters (HNP'B sheet Polaroid) with transmission axes at  $0^\circ$ ,  $45^\circ$ ,  $90^\circ$ , and  $135^\circ$ . We obtained 9 or 10 CCD images exposed for 800 seconds at each position angle for a total of 31,200 seconds of integration time. The data were taken during transparent but unphotometric conditions. Further details of our observing and data reduction technique are presented in McNamara et al. 1996.

## 3. Properties of the Central Dominant Galaxy

In Figure 1 we present a composite image of the A2597 CDGs blue lobes embedded in the smoothed, grayscale contours of the U-band image of the galaxy. The superposed white contours show the 8.44 GHz radio emission mapped with the VLA, presented earlier in Sarazin et al. (1995). The composite U-band image was constructed first by subtracting the model for the background galaxy discussed in Section 4.1 from the summed, 31.2 ksec U-band image, leaving the bright blue lobes in residual. The residual image was then multiplied by an arbitrary factor, and the U-band image was smoothed with a 4 pixel FWHM Gaussian kernel. The residual and U-band images were scaled logarithmically, added, and displayed in grayscale. This rendering allows the brightest and bluest regions in black to be seen against the background galaxy contours in gray and the radio source in white. The structure seen in earlier U and I data by MO93 and Sarazin et al. (1995) is clearly seen in our new U-band data, although the pixels in the new data subtend a larger angular size, and details on scales smaller than  $\simeq 2$  arcsec may be unreliable.

We will not repeat the detailed discussions of the galaxy's properties presented in MO93 and Sarazin et al. (1995), but we will mention a few salient properties pertaining to this discussion. The radio jets are seen in Figure 1 to emerge from the nucleus in a north-east/south-west direction along the minor photometric axis of the galaxy. The bright blue lobes, shown in black, are located near the radio lobes. They are brightest and bluest 2–3 arcsec from the nucleus, where the colors of the blue lobes are 0.7–1.0 magnitudes bluer in  $U - I$  than the colors of a normal giant elliptical at that radius. The most striking indication that the radio source and matter associated with the blue lobes are interacting is the sharp bend in the radio structure to the south-west, where the radio lobe seems to be expanding and bending at the location of the southern blue lobe. O'Dea, Baum, and Gallimore (1994) discovered H I in absorption against the radio lobes with a broad,  $\sim 410 \text{ km s}^{-1}$  FWHM, turbulent velocity structure whose mean velocity is consistent with the

mean velocity of the galaxy. Sarazin et al. (1995) suggested that the radio jets may have been deflected and the radio lobes disrupted as the outwardly moving radio plasma collided with the H I clouds. The H I clouds may be associated with the bright emission-line nebula embedded in the inner 20 kpc of the galaxy (O’Dea, Baum, and Gallimore 1994).

#### 4. Polarization Analysis

We determined the degree of polarization of the U-band light emitted from the entire central blue region and from the blue lobes individually. To do so, we extracted the net fluxes in these regions using circular synthetic apertures applied to the sum of the CCD frames for each transmission angle, after subtracting the sky background from each of the CCD frames. The Stokes flux for each aperture was computed by taking flux differences between transmission axes,  $S_\theta$ , as  $Q = S_{0^\circ} - S_{90^\circ}$ ,  $U = S_{45^\circ} - S_{135^\circ}$ . The normalized Stokes flux was found as  $q_n = Q/(S_{0^\circ} + S_{90^\circ})$  and  $u_n = U/(S_{45^\circ} + S_{135^\circ})$ , where the degree of instrumental plus total polarization was found as  $P = \sqrt{q_n^2 + u_n^2}$ . The degree of total polarization (background stars plus blue lobes) of the flux at each aperture position on the galaxy was found by subtracting the mean instrumental polarization determined using the presumably intrinsically unpolarized flux for eight reference objects in the field surrounding the central galaxy as  $P_{\text{tot}} = P_{\text{gal}} - P_{\text{ref}}$ .

A summary of the polarization measurements and the sizes and locations of the apertures are given in Table 1. Columns 1–3 give the locations of the aperture centers with respect to the nucleus, defined as the peak in the U-band flux. The offsets from the nucleus are given in column 2, and the position angles measured from north through east are given in column 3. Column 4 lists the diameters of the circular apertures. Column 5 lists the total polarization found in each aperture, and column 6 gives the RMS deviations about the mean instrumental polarizations for the eight reference objects. Column 7 lists the upper limits to the degree of polarization of the blue lobe light in each aperture, after correcting for background light. The procedure we used to derive the data listed in column 7 is described in Section 4.1. In column 8, we list the net polarization after accounting for dilution by the stellar background (i.e. column 7) and nebular emission (§4.2).

An inspection of columns 5 and 6 in Table 1 shows no significant total polarization for the large central aperture or the smaller apertures circumscribing the blue lobes. The upper limits to the degree of polarization of the total light from the lobes (lobes + galaxy) is less than 2%, based on the scatter in the measured degree of instrumental polarization of the reference objects. The statistical error in the each of the Stokes parameters, which included variations in the U-band sky background ( $\leq 1\%$ ) and photon statistics ( $\ll 1\%$ ), was found to be less than 1%.

#### 4.1. Stellar Background Model

In order to determine the upper limits to the intrinsic polarization of the blue lobes, we modeled and removed the contribution of presumably unpolarized starlight from the galaxy. The background galaxy model was constructed by first measuring the U-band radial surface brightness profile of the galaxy. This profile was constructed by extracting fluxes from elliptical annuluses with shapes defined by the I-band major axis position angles and isophotal ellipticities, based on data from McNamara & O’Connell (1993). The radial surface brightness model was constructed by fitting a straight line to the U-band radial surface brightness profile in magnitudes per square arcsec against semimajor axis to the 1/4-power. This  $R^{1/4}$ -law profile was fit to the data at radii between 13 and 20 arcseconds, well beyond the the blue central region of the galaxy where the colors are apparently typical of a normal cD galaxy. The surface brightness profile is shown as solid dots, and the fitted  $R^{1/4}$ -law profile is shown as a solid line in Figure 2. The model profile is extrapolated inward in order to construct the model of the older background population at the location of the lobes. The departure of the observed surface brightness profile above the  $R^{1/4}$ -law profile is clearly seen in the inner 8 arcsec or so where the excess blue light and line emission are observed (McNamara & O’Connell 1993; Sarazin et al. 1995; Cardiel, Gorgas, & Aragon-Salamanca 1997). The  $R^{1/4}$ -law profile overestimates the contribution of background light in the inner arcsec or so of the galaxy. This should have little effect on the estimated contribution of background light at the locations of the blue lobes. The model surface brightness profile was then applied to the corresponding semimajor axis locations in the artificial image of the galaxy whose shape was identical to the mean isophotal shape of the I-band image of the galaxy.

The contribution of background light at the locations of the apertures placed on the image of the real galaxy was found by measuring the flux in the model galaxy using identical apertures and locations as for the real galaxy and reference objects (i.e. Table 1). The Stokes parameters and degree of polarization of the net flux from the lobes after subtracting the galactic stellar model background,  $f_{M(r)}$ , were found as  $q = Q/(S_{0^\circ} + S_{90^\circ} - f_{M(r)})$ ,  $u = U/(S_{45^\circ} + S_{135^\circ} - f_{M(r)})$ ,  $P = \sqrt{q^2 + u^2}$ , and  $P_* = P_{gal} - P_{ref}$ .

The values of  $P_*$  found for each aperture are given in column 7 of Table 1. They show that the three sigma upper limit to the degree of polarization of the net flux from the lobes is less than 5%. The three sigma limit was computed by adding an offset to the surface brightness model profile equal to three times the statistical error in the zero point of the  $R^{1/4}$ -law fit to the data, and then following through with the analysis of the model data as described above. The RMS error associated with the measurement of the total polarization prior to considering the background model is less than 2%. Therefore, dilution by ambient starlight surrounding the blue lobes is the factor limiting the precision of the polarization measurement. The  $3\sigma$  upper limit to the total polarized flux (lobe + galaxy) of both lobes at  $U$  is  $< 1.7 \times 10^{-15}$  erg cm $^{-2}$  s $^{-1}$ . This figure was estimated using calibrated photometry (McNamara & O’Connell 1993; Sarazin et al. 1995), and the upper limit of 2% to the degree of polarization of the total light at  $U$  presented here.

## 4.2. Nebular Emission

Diffuse Nebular line emission in the vicinity of the A2597 CDGs blue lobes is quite strong (Voit & Donahue 1997), and the contributions of diffuse nebular continuum and line radiation to the U-band could be significant. Unpolarized nebular radiation would dilute a polarized signal.

In order to determine the fraction of the U-band color excess that may be attributable to unpolarized nebular continuum, we estimated the amount of recombination radiation from hydrogen and helium, two photon emission, and bremsstrahlung radiation that would be expected for the conditions in A2597. We calculated these emissions relative to the strength of the H $\beta$  emission line using the Case B emission coefficients tabulated in Aller (1984) and Osterbrock (1974). The contribution of nebular continuum to the  $U - B$  color excess in the vicinity of the blue lobes can be described then as,

$$\Delta(U - B) \simeq -2.5 \log \left[ 1 + \frac{\epsilon(T, \Delta\lambda_U)EW(\text{H}\beta)}{\Delta\lambda_U} \right]. \quad (1)$$

In this expression,  $EW(\text{H}\beta)$  is the equivalent width of the H $\beta$  emission feature,  $\Delta\lambda_U \simeq 600$  Å is the approximate effective width of the  $U$  passband, and  $\epsilon(T, \Delta\lambda_U)$  is the ratio of the strength of the nebular continuum averaged over the  $U$  passband to the H $\beta$  line flux. We assumed half solar abundances, a gas density of  $200 \text{ cm}^{-3}$ , and an ion temperature of 10,000 K, appropriate to the nebula surrounding the blue lobes (Voit & Donahue 1997). The strength of the nebular continuum does not depend significantly on the ion density for the densities of interest here, but it does depend somewhat on ion temperature. We have adopted  $\epsilon = 2.8$  to be consistent with the Voit & Donahue (1997) analysis. We are unaware of a tabulated measurement in the literature of the H $\beta$  equivalent width for the A2597 CDG in the vicinity of the blue lobes. Therefore, we estimated the H $\beta$  equivalent width to be  $EW(\text{H}\beta) = 28$  Å in the nucleus using the tabulated H $\beta$  flux and the continuum spectrum given in Voit & Donahue (1997). Cardiel et al. (1998) measured the radial profile of the H $\beta$  equivalent width and similarly found it to be 28 Å in the nucleus, after correcting for H $\beta$  absorption. They found that equivalent width decreases with radius to  $\simeq 15 - 23$  Å at the radius of the blue lobes. Unfortunately Cardiel’s measurements were made using a slit placed perpendicular to the blue lobes along the major axis of the galaxy, so we do not know the precise value of the H $\beta$  equivalent width at the location of the lobes. We find that the color excess at the location of the blue lobes that can be attributed to unpolarized nebular continuum is  $\Delta(U - B) \gtrsim -0.07$  to  $-0.11$  magnitudes. This color excess corresponds to H $\beta$  equivalent widths of 20Å and 30Å respectively, which bracket the values in the nucleus and at the radius of the blue lobes. The upper bound on the color excess contributed by unpolarized nebular emission should be reasonable because the nebular emission is centrally concentrated (Heckman et al. 1989), and our estimate exceeds the nuclear value. Nonetheless, our estimate should be taken with due caution, absent a direct measurement, as the H $\beta$  equivalent width could be larger near the blue lobes than we have assumed. The observed total color excess in A2597’s lobes is  $\Delta(U - B) \simeq -0.6$

magnitudes (McNamara 1997; Cardiel, Gorgas, & Aragon-Salamanca 1997). Therefore, we expect the unpolarized nebular continuum to comprise only  $\simeq 10 - 15\%$  of the observed total color excess.

The uncertainty in the measurement of the total color excess is caused primarily by the unknown dust distribution within the nebula. Voit & Donahue (1997) found  $\simeq 0.3$  magnitudes of extinction at  $U$  based on departures of observed Balmer line ratios from Case B predictions. This extinction should not affect appreciably our estimate of the percentage of the color excess that is contributed by nebular and stellar continuum unless the gas, dust, and young stars are distributed differently. The existing data do not allow us to determine whether this is so.

The equivalent width of A2597's [O II] $\lambda$ 3727 emission feature is  $\simeq 247 \text{ \AA}$  in the nucleus (Voit & Donahue 1997). However, assuming the [O II] equivalent width decreases with radius proportionally to the  $H\beta$  feature, we expect the [O II] equivalent width at the location of the lobes to be roughly between 130–200  $\text{\AA}$ . The [O II] feature's location is redshifted to  $\lambda$ 4034  $\text{\AA}$  in the laboratory frame, where the throughput of the U-band filter is about 5%. We estimate the contribution of [O II] emission to the  $U$  band at the location of the lobes to be between 0.01–0.02 magnitudes, or about 3% of the color excess.

In summary, we estimate the total nebular contribution to the  $U$ -band color excess, including [O II] emission plus nebular continuum, to be between 13–18%. This continuum would dilute a polarized signal from the blue lobes and increase the upper limits to the degree of polarization by one percent or less (i.e.  $P_{*,\text{neb}}$ , Table 1, column 8).

## 5. Radiation Mechanisms for the Blue Lobes

### 5.1. Interpretation of the Polarization Upper Limits

We now calculate the expected polarization of the blue lobes in A2597 if they are due to electron scattering or dust scattering, and compare to the observed upper limit. The expected linear polarization of the blue lobes in the A1795 CDG due to electron scattering by the cooling flow was calculated by Sarazin & Wise (1993) and was discussed in detail in McNamara et al. (1996a). The blue lobes in A2597 are similar in many respects, and our analysis follows that for A1795 (McNamara et al. 1996a). We assume that the blue lobes are due to scattering of beamed radiation. We consider beamed rather than isotropic emission because no strong nuclear point source is seen in A2597 (Crawford & Fabian 1993; Sarazin & Wise 1993). The model polarization was calculated for the scattered light only, without dilution by the background galaxy light.

First, we consider the possibility that the blue lobes are due to electron scattering. We assume single electron scattering, as the observed electron scattering optical depth of the cooling flow is small (Sarazin et al. 1995). In this limit, the polarization is independent of the scale of the

electron density of the cooling flow. Of course, the polarization is always independent of the flux of the anisotropic nuclear source.” The assumptions included in our scattering model are identical to those discussed in McNamara et al. (1996a), with the exception of the opening angle of the scattering cones. We assume that the electron density,  $n_e$ , in the cooling flow varies with radius,  $r$ , as  $n_e \propto r^{-1}$ , which gives a reasonable fit to the observed X-ray surface brightness at small radii (Sarazin et al. 1995).

For this calculation, we assume that anisotropic radiation from the central nucleus is conical, initially unpolarized, and uniformly illuminated. The polarization is calculated including the effects of averaging along the line-of-sight through the beam and averaging the azimuthal polarization across the projected width of the beams. The polarization depends slightly on the observed width of the lobes. We estimate an angular half-width of  $\phi_{max} \approx 35 - 45^\circ$  for the NE lobe and  $\phi_{max} \approx 25 - 35^\circ$  for the SW lobe. We adopt  $\phi_{max} = 35^\circ$ , but note that the resulting polarization is not strongly dependent on this assumption or any of the other assumptions, as shown in Sarazin & Wise (1993) and McNamara et al. (1996a). The predicted polarization does depend strongly on the angle  $\theta$  between our line-of-sight and the central direction of the beams. (See Figure 1 in Sarazin & Wise [1993] for the definitions of the angles.) For each value of the angle  $\theta$ , we determine the angular width of the beams  $\theta_b$  which is consistent with the observed width  $\phi_{max}$  of the blue lobes in A2597. The existence of distinct lobes and the fact that the nucleus is not extremely bright both require that our line of sight be outside of the beams, so that  $\theta_b < \theta$ .

Figure 3 shows the predicted polarization (solid line) of the electron-scattered lobe light,  $P$ , as a function of the angle of the beams to the line-of-sight,  $\theta$ . The observed upper limit of  $P < 6\%$  is shown as a long dashed horizontal line. The observed upper limit is only consistent with the prediction of the simple electron scattering model if  $\theta < 20^\circ$ . The probability,  $P_o$ , that the beam would be randomly oriented this close to our line-of-sight is  $P_o < 6\%$ . (Note that for small polarizations, the probability and the polarization are always nearly equal.) Thus, the consistency of the observed upper limit on the polarization of the lobes with the simple electron scattering model would require an unlikely near alignment of the beams with our line of sight. A very similar result was found for the blue lobes in A1795, where the limit on the orientation angle and probability were  $\theta < 22^\circ$  and  $P_o < 7\%$ . The strong upper limits on the polarization of the lobes makes it unlikely that they are due to electron scattering. While a single case might be the result of an unlucky alignment, it seems very unlikely that both could be explained this way.

This calculation of the polarization in Figure 3 assumed that the emission from the nucleus of the AGN was unpolarized. If the nucleus contains a BL Lac object, then the nuclear emission might itself be highly polarized. In most situations, this will increase the polarization of the scattered light (Sarazin & Wise 1993). However, for certain very restrictive choices of the angles, the polarization can decrease, although this requires that the parameters be at least as finely tuned as in the case for scattering of unpolarized radiation (McNamara et al. 1996a).

We have also calculated the predicted polarization for scattering by dust. We assumed the dust scattering properties given by White (1979) for the standard MRN model for interstellar dust. The predicted polarization for dust scattering is shown by the short dashed curve in Figure 3. Unlike electron scattering, dust scattering is not symmetric between forward and backward scattering, and thus the two lobes would have different polarization. Since neither of the two observed lobes shows any evidence of polarization, the curve shown is the maximum of the polarizations of the two lobes. At small and large values of  $\theta$ , the polarization is larger for the back lobe (the one further away from us, for which the scattering is predominantly back scattering). At intermediate angles ( $37^\circ \leq \theta \leq 61^\circ$ ) the polarization of the front lobe is higher. At small angles ( $\theta < 37^\circ$ ), the predicted polarization due to back scattering is radial for the more strongly polarization lobe. At all other angles, the predicted polarization is azimuthal. (The polarization due to electron scattering is always azimuthal for an initially unpolarized source.)

For both A1795 and A2597, the lack of observed polarization in the lobes and the fact that they are not very strongly asymmetric in their brightness makes it unlikely that they are due to dust scattering. The polarization produced by dust scattering is smaller than that produced by electrons. As a result, the limit on the angle  $\theta$  is weaker. The observed limit on the polarization of less than 6% implies that  $\theta \leq 22^\circ$  or  $30^\circ \leq \theta \leq 44^\circ$ , for which the probability is  $P_o \leq 23\%$ . However, dust scattering is not symmetric forward to back, and the same conditions which would lower the polarization (small  $\theta$ ) would produce rather asymmetric lobes, with a ratio of fluxes which would exceed  $\geq 6$ . While the two lobes are certainly not symmetric, the ratio of their surface brightnesses is  $\lesssim 4$  (Sarazin et al. 1995). We have also determined the predicted polarization due to dust scattering in A1795 (McNamara et al. 1996a). There, the 3- $\sigma$  upper limit polarization leads to an upper limit on the angle of  $\theta \leq 46^\circ$ , a probability of  $P_o \leq 31\%$ , and a flux ratio of  $\geq 5.8$ .

Given these limits on dust scattering and the stronger limits on electron scattering, it is improbable that the lobes are due scattering of beamed light from the nuclei of the galaxies. The absence of a polarized signal or of a detailed correspondence between the radio and optical morphologies renders synchrotron radiation an unlikely emission mechanism. Furthermore, Compton scattering of microwave background photons by relativistic electrons associated with the radio source (c.f. Daly 1992) is incompatible with the object’s proximity and radio power, and optical bremsstrahlung radiation from the diffuse X-ray source would be too weak to explain the blue lobes for the observed gas densities in A2597 (Sarazin et al. 1995).

Finally, our polarization measurements probe directly the paradigm that seeks to unify FR I radio sources and BL Lac objects (e.g. Urry and Padovani 1995). The A2597 and A1795 CDGs reside in hot cluster atmospheres with central gas densities of  $\sim 10^{-1} \text{ cm}^{-3}$ . Were the CDGs to contain typical BL Lac nuclei,  $\sim 1\%$  of the anisotropically emitted radiation from the BL Lac would be scattered off of electrons into the line of sight, which should be detectable (Sarazin & Wise 1993). Furthermore, the alignment of the blue lobes with the radio sources (McNamara & O’Connell 1993) is consistent with the scattering hypothesis, which prompted Sarazin and Wise to investigate its feasibility. Their scattering model assumes anisotropic nuclear emission

directed obliquely to the line of sight, with luminosities comparable to a typical BL Lac object ( $L = 10^{47}$  ergs  $s^{-1}$ ) in the spectral range  $\Delta\nu = 10^8 - 10^{18}$  Hz. The scattering medium was assumed to be an electron gas of comparable density to the X-ray-determined values at the centers of the cooling flows. The predicted  $U$ -band surface brightness of the scattered light matched closely the observed surface brightness of the lobes in A2597 and A1795 found by McNamara & O’Connell (1993). However, the remaining critical question was the degree of polarization of the  $U$ -band lobe emission, which should be  $> 8\%$  were the blue lobes scattered light. The polarization measurements presented here were intended to test the scattering model. Our upper limits are then inconsistent with the scattering model and do not support the FR I–BL Lac unification paradigm to the extent that the assumptions made by Sarazin & Wise (1993) are reasonable.

## 5.2. Radio Triggered Star Formation

Following on the previous section, we conclude that the radiation from blue lobes is most likely primarily continuum from young, blue stars. This interpretation receives further support by a recent analysis of the nebular emission surrounding the lobes (Voit & Donahue 1997). The spatial correlation between the blue lobes and radio lobes shown in Figure 1, McNamara & O’Connell (1993), and Sarazin et al. (1995) suggests that the blue lobes and the radio source are related either by chance: the radially expanding radio jets happened upon the dense clouds associated with the blue, star-forming regions, or causality: the star formation was triggered by the radio source. A mere coincidence seems unlikely. There is one other obvious example of this phenomenon in the A1795 CDG, which, as A2597, was identified among the roughly two dozen or so clusters with large cooling flows whose CDGs have been well imaged from the ground (McNamara 1997). The bluest and presumably the youngest regions of star formation have been shown, using HST imagery, to lie along the edges of the radio lobes in A1795 (McNamara et al. 1996; Pinkney et al. 1996). Although the bluest regions in A2597 are located near the radio lobes (i.e. Figure 1), HST images show that they do not correlate strongly with the edges of the radio lobes (Koekemoer et al. in preparation), as is seen in A1795. Although this would render A2597 a less compelling case for radio-triggered star formation, the mechanism by which star formation is induced is poorly understood, and predictions based on such models are uncertain.

De Young (1995) presented a model to explain the lobes in A1795 as a burst of star formation triggered by the rapid collapse of cold clouds compressed by shocks along the expanding radio jets. This general scenario is consistent with bends in the radio sources of both objects occurring near regions of dust extinction,  $H\alpha$  emitting gas, and in A2597, near H I absorption clouds (McNamara et al. 1996; O’Dea et al. 1994; Koekemoer et al. in preparation), which indicates that the radio sources are interacting with cold gas clouds. However, De Young’s model does not readily explain the location of the bluest, and presumably the youngest star clusters along the edges of the radio lobes in A1795, rather than along the edges of the jets.

The weaker correlation between the bluest regions and the radio source in A2597 is not necessarily surprising. A strong correlation between the edges of the radio source and the sites of star formation should be short lived (McNamara & O’Connell 1993; De Young 1995; McNamara et al. 1996a; Cardiel, Gorgas, & Aragon-Salamanca 1997). The nebular and H I gas velocities of a few hundred kilometers per second near the lobes are disordered (Heckman et al. 1989; O’Dea et al. 1994). Assuming the star formation is fueled by cold gas with a similar velocity structure, the stellar lobes should disperse quickly, and certainly in less than the local free-fall time of a few tens of Myr. Therefore, it is possible that we have caught the burst of star formation in A2597 several Myr after it was initiated by the radio source, and stars have begun to disperse as the radio source expands outward.

The ground-based photometry and radio data are not capable of pinpointing the relative ages of the radio source and regions of star formation to reliably test this hypothesis. Nonetheless, the short dispersal timescale would be consistent with both the lower limit on the radio age of 0.5 Myr (Sarazin et al. 1995) and with the colors for a burst of star formation that occurred roughly 5 Myr ago with the local initial mass function and solar abundances (McNamara & O’Connell 1993). The stellar mass of the blue lobes composed of such a population would be  $\sim 10^8 M_{\odot}$ , which implies a total star formation rate in both lobes of roughly  $20 M_{\odot} \text{ yr}^{-1}$ . This star formation rate and stellar mass does not include adjustments upward for extinction, and adjustments downward for nebular emission (§5.3). Including a  $\Delta(U - B) \simeq -0.3$  magnitude extinction correction, and a  $\Delta(U - B) \simeq +0.1$  magnitude nebular emission correction, the young stellar mass and star formation rate would increase by about 68%. This systematic increase does not exceed the uncertainties of the estimate of the uncorrected mass, which matches reasonably well with the mass of neutral hydrogen of  $\sim 7 \times 10^7 M_{\odot}$  estimated from the VLA H I absorption measurements (O’Dea et al. 1994).

## 6. A Comparison Between the Polarized Luminosities and Radio Power for Radio Aligned CDGs and High Redshift Radio Galaxies

In this section we explore the similarities and differences between the alignment properties of the high redshift radio galaxies (HzRGs) and those in A2597 and A1795. We wish to determine whether they are fundamentally different types of object, or whether they are similar albeit on much different spatial and energy scales. In order to do so, we will begin by contrasting a few of their relevant properties, most importantly their polarized luminosities and radio powers.

The blue optical continuum found along the radio sources in HzRGs is often polarized at levels of several to greater than ten percent. The electric vectors are, in general, nearly perpendicular to the radio and optical continuum axes. In addition, they have strong, extended, nebular line emission near their radio sources. Based on these facts, a consensus has emerged that would explain

the aligned optical continuum as being primarily scattered light from a powerful, misdirected active nucleus or QSO, plus a smaller but significant contribution of nebular continuum (e.g. Dey 1998; Cimatti et al. 1997; Dey et al. 1996; Stockton, Ridgway, & Kellogg 1996; Dickson et al. 1995). While this may be the case in the majority of aligned HzRGs with reliable polarimetry, it is not always true. For example, the aligned components in 3C 285 (van Breugel & Dey 1993) and 4C 41.17 (Dey et al. 1997) are unpolarized. Their aligned continua appear to originate from young stellar populations. Furthermore, even in those objects with a high degree of polarization, star formation at some level cannot always be excluded (Cimatti et al. 1996). Therefore, there appear to be at least three physical processes corresponding to three emission mechanisms that contribute to the alignment effect in HzRGs: scattered light, nebular continuum, and star formation.

In contrast, the alignment seen in A2597 is associated with a smaller, lower power, FR I radio source. Its radio-aligned, *U*-band optical continuum is composed primarily of light from a young,  $\sim 10$  Myr old stellar population ( $\gtrsim 80\%$ ), a small contribution of nebular emission ( $\sim 10 - 20\%$ ), and at most a minor contribution of scattered light. The situation is similar in the A1795 CDG (McNamara et al. 1996a). In addition, the blue optical emission found near the radio lobe of the FR I radio source PKS 0123-016A, the well-known “Minkowski’s Object,” is primarily from a young stellar population (van Breugel et al. 1985). Therefore, both star formation, and to a small degree nebular emission, contribute to the aligned optical components in the FR Is. However, we are unaware of any evidence of scattered radiation playing a major role in producing the aligned optical components of an FR I radio galaxy.

The environments of the FR I radio sources in the A2597 and A1795 central cluster galaxies and HzRGs that exhibit the alignment effect are similar in at least three general but important respects. Both types of radio source seem to be found in elliptical host galaxies (Rigler et al. 1992; Cimatti et al. 1994; Dey 1998). Second, one can infer by the presence of radio sources that they contain a central engine that powers their radio sources. Third, by virtue of the presence of strong nebular line emission and recent star formation, the host galaxies must harbor reservoirs of cool gas (e.g. McNamara 1997 and references therein). A2597 and A1795 are dissimilar to the powerful HzRGs, lacking evidence for bright, blue, unresolved continua in their nuclei (e.g. McNamara et al. 1996b; Pinkney et al. 1996) or broad emission lines (Heckman et al. 1989).

The characteristic that perhaps best distinguishes between A2597, A1795, and the HzRGs is radio power. We calculated the radio powers for several high redshift 3C radio galaxies observed with the Keck Observatory (e.g. Dey 1998). The radio powers in the restframe 1.4 GHz bandpass,  $P_{1.4}$ , were found by interpolating between measured flux densities bracketing the restframe frequency  $\nu = 1.4/(1+z)$  GHz. We have assumed  $H_o = 50 \text{ km s}^{-1} \text{ Mpc}^{-1}$  and  $q_0 = 0.5$  throughout our calculations. The computed flux densities and radio powers are presented in Table 2. In columns 1 and 2 we list the radio galaxy name and redshift. Column 3 lists the restframe radio flux density; column 4 lists the restframe radio power; column 5 lists the degree of polarization in the restframe U passband, determined from spectropolarimetry obtained with the Keck Observatory. In column 6 we list the restframe U-band polarized continuum luminosity. The

polarized luminosity was determined as

$$L(U)_{\text{pol}} = 4\pi D_{\text{lum}}^2 f_{\lambda 3600} \Delta\lambda_U P(U), \quad (2)$$

where  $f_{\lambda 3600}$  is total flux at 3600 Å, and  $P(U)$  is the degree of polarization at 3600 Å in the rest frame. The effective rest frame  $U$  passband is assumed to be  $\Delta\lambda_U = 600$  Å, and  $D_{\text{lum}}$  is the luminosity distance to the radio galaxy. In column 7 we index the references to the data. We have included entries in Table 2 for A2597 and A1795 for comparison. Because we computed the polarized luminosities and radio powers of the HzRGs in the restframe U-band, they can be compared directly to those for A2597 and A1795.

The radio power is plotted against the restframe U-band polarized continuum luminosity in Figure 4. Note the difference of a factor of several thousand in radio luminosity between the A2597, A1795, and the aligned HzRGs. In addition, the polarized luminosities of the HzRGs are  $\sim 600\times$  larger than the upper limits for the FR Is. In all likelihood, the much larger radio powers in HzRGs are the result of a much stronger AGN. Consequently, the HzRGs are capable of producing a much higher scattered light intensity for a given ambient electron or dust density. Now we ask whether we would have detected any polarized flux in A2597 and A1795 if the polarized luminosity scales in proportion to the radio power. The solid line in Fig. 4 represents  $L(U)_{\text{pol}} \propto P_{\text{rad}}$ . The line is scaled to the median of the 3C radio galaxies. We can see that the ratio of polarized luminosity to radio power for the HzRGs extrapolated downward to the radio power of the aligned FR Is falls a factor of about 30 below the upper limits for A1795 and A2597. Therefore, if  $L(U)_{\text{pol}} \propto P_{\text{rad}}$  our polarimetry for A2597 and A1795 would not have detected the polarized signal. The composition (electrons, cold gas, dust), density, and spatial distribution of the interstellar medium of the host galaxy, and the orientation of the AGN are factors that would contribute scatter to the relationship plotted in Figure 4. However, by using several, well-observed 3C galaxies, we have attempted to average over these factors. In any case, when the line is scaled to the upper envelope of the group of 3C galaxies in Figure 4, the A2597 and A1795 upper limits remain well above the line. Therefore, we conclude with reasonable confidence that were the AGN in the A1795 and A2597 CDGs the dwarf siblings of the aligned HzRGs, we would not have detected their polarized signals. This result depends on the adopted cosmology in detail, but the conclusion is unaffected.

Our conclusion rests uncomfortably on an extrapolation of 3–4 orders of magnitude in radio power and a factor of 600 in polarized luminosity. It would be reassuring to find and explore alignment effect radio galaxies that lie between the FR I and HzRGs in Figure 4. Furthermore, if A1795 and A2597 indeed contain weak AGN similar in nature to the HzRGs, a polarized signal of  $\sim 2 \times 10^{-16}$  erg cm<sup>-2</sup> sec<sup>-1</sup> should be present, if our extrapolation to low radio power is correct. This flux is roughly an order of magnitude below our limits for A1795 and A2597. However, a polarized flux at this level may be detectable near the nucleus using high resolution space polarimetry, or ground-based polarimetry using a large telescope in excellent seeing.

Finally, we highlight earlier remarks that pure Thompson scattering models imply the

presence of large cooling flows in HzRGs (Cimatti et al. 1994). This suggestion is supported by the detection of possibly extended, luminous X-ray emission surrounding some HzRGs (e.g. 3C356; see Crawford (1997) for a recent review). The possibility that some HzRGs may be located at the base of distant cooling flows would be an additional thread tying together the HzRGs and the low redshift cooling flows. In addition to supplying a scattering medium, cooling flows are capable of fueling star formation and the central engine.

## 7. Conclusions

We have found a three-sigma upper limit to the degree of polarization of the  $U$ -band light emitted from A2597's blue lobes to be less than 6%. This limit includes corrections for dilution by background starlight and nebular emission. The  $U$ -band emission from the blue lobes is composed of 75 – 88% stellar continuum from young stars, 13 – 18% nebular emission, and less than 6% scattered light. Earlier studies of the CDG in A1795 (McNamara et al. 1996a,b), which has similar properties to the CDG in A2597, came to similar conclusions.

Our limits do not support the conjecture that the blue lobes are scattered light from an obscured BL Lac or blazar nucleus associated with the FR I radio source PKS 2322–122. However, if the beamed AGN luminosity and hence the polarized luminosity scales with radio luminosity, the FR I radio galaxies in A2597 and A1795 could be scaled-down versions of the high redshift radio galaxies exhibiting the alignment effect. AGN that would be present in these objects must have low  $U$ -band luminosities. The asymmetries in the radio structures of the A1795 and A2597 CDGs may have resulted from interactions between the radio jets and dense, dusty clouds encountered by the jets. The star formation associated with the blue lobes may have been triggered by these interactions.

We thank Nicolas Cardiel for providing us with  $H\beta$  equivalent widths. B. R. M. was supported by grant NAS8-39073 to the Smithsonian Astrophysical Observatory. C. L. S. thanks Bill Sparks for a very useful conversation. C. L. S. was supported in part by NASA Astrophysical Theory Program grant 5-3057 and NASA ROSAT grants NAG 5-4787 and NAG 5-3308.

Table 1: Polarization Measurements

Location	$r$ (arcsec)	PA (degrees)	$A_p$ (arcsec)	$P_{\text{tot}}$ (%)	$\sigma_p$ (%)	$P_*$ (%)	$P_{*,\text{neb}}$ (%)
Nucleus	...	...	10.4	−0.9	1.4	< 4.9	< 5.8
NE Lobe	2.7	45	4.70	0.5	2.0	< 4.8	< 5.7
SW Lobe	3.4	236	4.70	−1.5	2.0	< 2.9	< 3.4

## REFERENCES

- Aller, L.H. 1984, *Physics of Thermal Gaseous Nebulae* (Dordrecht: Reidel), 115, 98
- Antonucci, R. 1993, *ARAA*, 31, 473
- Baum, S.A. 1992, in *Clusters and Superclusters of Galaxies*, ed. A.C. Fabian, (Dordrecht: Kluwer), 171
- Becker, R.H., White, R.L., Edwards, A.L. 1991, *ApJS*, 75, 1
- Begelman, M.C., & Cioffi, D.F. 1989, *ApJ*, 345, L21
- Bohren, C. F., & Huffman, D. R. 1983, *Absorption and Scattering of Light by Small Particles* (New York: Wiley)
- Cardiel, N., Gorgas, J., Aragon-Salamanca, A. 1997, *MNRAS*, submitted
- Cardiel, N., Gorgas, J., Aragon-Salamanca, A. 1998, in preparation.
- Chambers, K.C., Miley, G.K., & van Breugel, W. 1987, *Nature*, 329, 604
- Cimatti, A., di Serego Alighieri, S. 1995, *MNRAS*, 273, L7
- Cimatti, A., di Serego Alighieri, S., Field, G.B., Fosbury, R.A.E. 1994, *ApJ*, 442, 562
- Cimatti, A., Dey, A., van Breugel, W., Hurt, T., Antonucci, R., 1997, *ApJ*, 476, 677
- Cimatti, A., Dey, A., van Breugel, W., Antonucci, R., Spinrad, H. 1996, 465, 145
- Crawford, C.S. 1997, in *Galactic and Cluster Cooling Flows*, ed. N. Soker, (San Francisco: Publ. Astr. Soc. Pacific), 38
- Daly, R.A. 1990, *ApJ*, 355, 416
- Daly, R.A. 1992, *ApJ*, 386, L9
- Dey, A. 1998, to be published in “The Most Distant Radio Galaxies”
- Dey, A., Cimatti, A., van Breugel, W., Antonucci, R., & Spinrad, H. 1996, *ApJ*, 465, 157
- Dey, A., van Breugel, W., Vacca, W.D., Antonucci, R. 1997, *ApJ*, 490, 698
- De Young, D.S. 1989, *ApJ*, 342, L59
- De Young, D.S. 1995, *ApJ*, 446, 521
- Dickson, R., Tadhunter, C., Shaw, M., Clark, N., Morganti, R., 1995, *MNRAS*, 273, L29
- di Serego Alighieri, S., Fosbury, R.A.E., Quinn, P.J., & Tadhunter, C.N. 1989, *Nature*, 341, 307
- di Serego Alighieri, S., Cimatti, A., & Fosbury, R.A.E. 1993, *ApJ*, 404, 584
- di Serego Alighieri, S., Cimatti, A., & Fosbury, R.A.E., Perez-Fournon, I. 1996, *MNRAS*, 299, L57
- Fabian, A.C. 1989, *MNRAS*, 238, 41p
- Ficarra, A., Grueff, G., Tomassetti, G. 1985, *AA Suppl*, 59,255
- Heckman, T.M., Baum, S.A., van Breugel W.J.M., & McCarthy, P.J. 1989, *ApJ*, 338, 48
- Jannuzi, B.T. & Elston, R. 1991, *ApJ*, 366, L69
- Jannuzi, B. T., Elston, R., Schmidt, G. D., Smith, P. S., and Stockman, H. S. 1995, *ApJ*, 454, L111
- Jannuzi, B. T. 1994, in *I.A.U. Symposium No. 159, Multi-Wavelength Continuum Emission of AGN*, ed. T. J. - L. Courvoisier & A. Blecha, (Dordrecht; Kluwer), 470
- McCarthy, P.J. 1993, *ARAA*, 31, 639
- McNamara, B.R., & O’Connell, R.W. 1993, *AJ*, 105, 417 (MO93)

- McNamara, B.R., Jannuzi, B.T., Sarazin, C.L., Elston, R., & Wise, M. 1996a, *ApJ*, 469,66
- McNamara, B.R., Wise, M., Sarazin, C.L., Jannuzi, B.T., & Elston, R. 1996b, *ApJ*, 466, L9
- McNamara, B.R., O’Connell, R.W., & Sarazin, C.L. 1996c, *AJ*, 112, 91
- McNamara, B.R., 1997, in *Galactic and Cluster Cooling Flows*, ed. N. Soker, (San Francisco: Publ. Astr. Soc. Pacific), 109
- Murphy, B.W., & Chernoff, D.F., 1993, *ApJ*, 418, 60
- O’Dea, C.P., Gallimore, J.F., & Baum, S.A. 1995, *AJ*, 109, 26
- Osterbrock, D.E. 1974, *Astrophysics of Gaseous Nebulae*, (San Francisco: Freeman), 69
- Padovani, P. & Urry, C.M. 1990, *ApJ*, 356, 75
- Pilkington, J.D., Scott, P.F. 1965, *MNRAS*, 69, 183
- Pinkney, J., Holtzman, J.A., Garasi, C., et al. 1996, *ApJ*, 468, L13
- Rees, M.J. 1989, *MNRAS*, 239, 1p
- Rigler, M.A., Lilly, S.J., Stockton, A., Hammer, F., & Le Fevre, O. 1992, *ApJ*, 385, 61
- Sarazin, C.L., & Wise, M.W. 1993, *ApJ*, 411, 55
- Sarazin, C.L., Burns, J.O., Roettiger, K., & McNamara, B.R. 1995, *ApJ*, 447, 559
- Scarrott, S.M., Rolph, C.D., & Tadhunter, C.N. 1990, *MNRAS*, 243, 5p
- Urry, C.M., Padovani, P. 1995, *PASP*, 107, 803
- van Breugel, W, Heckman, T., & Miley, G. 1984, *ApJ*, 276, 79
- van Breugel, W., Filippenko, A.V., Heckman, T., & Miley, G. 1985, *ApJ*, 293, 83
- van Breugel, W., & Dey, A. 1993, *ApJ*, 414, 563
- Voit, G.M., & Donahue, M. 1997, *ApJ*, 486, 242
- White, R. L. 1979, *ApJ*, 229, 954
- White, R. L., Becker, R.H. 1992, *ApJS*, 79, 331
- Wright, A. Otrupcek, R. 1990, *Parkes Catalog*, p
- Zellner, B. 1973, in *I.A.U. Symp. 52: Interstellar Dust and Related Topics*, ed. J. M Greenberg & H. C. Van de Hulst (Dordrecht: Reidel), 109

Table 2: Radio and Polarized Luminosities of Radio Galaxies

Object	$z$	$S_{1.4}$ (Jy)	$P_{1.4}$ (log[W Hz <sup>-1</sup> ])	$P(U)$ (%)	$L_{\text{pol}}(U)$ (10 <sup>42</sup> erg sec <sup>-1</sup> )	Refs
3C 13	1.351	5.56	28.81	10	25	1,7,10
3C 256	1.824	3.54	28.90	11	3.7	2,11
3C 265	0.811	12.98	28.68	10	8.9	3,7,12
3C 324	1.206	13.59	29.08	12	9.4	4,11
3C 356	1.079	7.96	28.75	8	6.6	1,7
3C 368	1.132	9.58	28.87	< 3	< 34	5,7,11
3C 441	0.707	11.55	28.50	3	2.2	5,13
A2597	0.082	2.02	25.79	< 6	< 0.15	8,9
A1795	0.064	0.97	25.23	< 6	< 0.04	6,8

- 1) Cimatti et al. (1997) 2) Dey et al. (1996)  
3) di Serego Alighieri et al. (1996) 4) Cimatti et al. (1996)  
5) Dey (1998) 6) McNamara et al. (1996)  
7) White & Becker (1992) 8) Heckman et al. (1989)  
9) this paper 10) Ficarra et al. (1985)  
11) Wright & Otrupcek (1990) 12) Becker et al. (1991)  
13) Pilkington & Scott (1965)

### Figure Captions

**Figure 1.** U-band composite grayscale image of the core of the A2597 CDG, constructed as described in Section 3. The superposed white contours show the 8.44 GHz radio continuum map. The blue lobes, shown in black, are coincident with the radio continuum. North is at top, east is to the left.

**Figure 2.** The U-band surface brightness profile (solid circles) in magnitudes per square arcsec, with an arbitrary offset, plotted against semimajor axis to the  $1/4$  power. The solid line represent the  $R^{1/4}$ -law surface brightness profile used to correct the polarization measures for dilution by surrounding starlight. The blue lobes are located where the surface brightness profile rises above the  $R^{1/4}$  profile.

**Figure 3.** The predicted degree of polarization,  $P$ , if the blue lobes are due to scattered light from double beams of radiation. The abscissa  $\theta$  is the angle between the center of the cones of radiation and our line-of-sight. The predicted polarization includes the effect of the finite width of the beams; it is averaged both along the line-of sight through each lobe and across the projected width of the lobes. The upper solid curve give the polarization if the lobes are due to electron scattering (or Rayleigh scattering by small particles). The lower short-dash curve is the predicted polarization if the lobes are due to scattering by normal interstellar dust. The lobes are asymmetric for dust scattering, and the curve gives the maximum polarization of the two lobes. The long-dash horizontal line gives the observed  $3\text{-}\sigma$  upper limit on the polarization of 6%.

**Figure 4.** Radio power is plotted against the polarized luminosity for alignment effect radio galaxies. The 3C radio galaxies are grouped to the upper right, and the upper limits to the polarized luminosity for A1795 and A2597 are in the lower left of the plot. The solid line, normalized to the median of the 3C points, represents  $L(U)_{\text{pol}} \propto P_{\text{rad}}$ . The vertical dashed line indicates approximately the transition between FR I and FR II radio luminosities.

Figure 1.

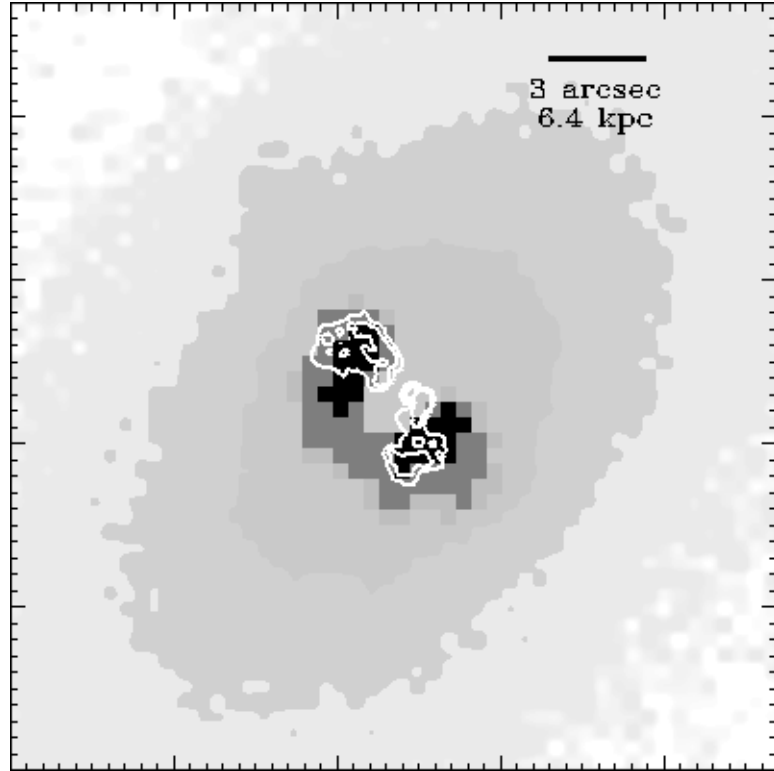


Figure 2.

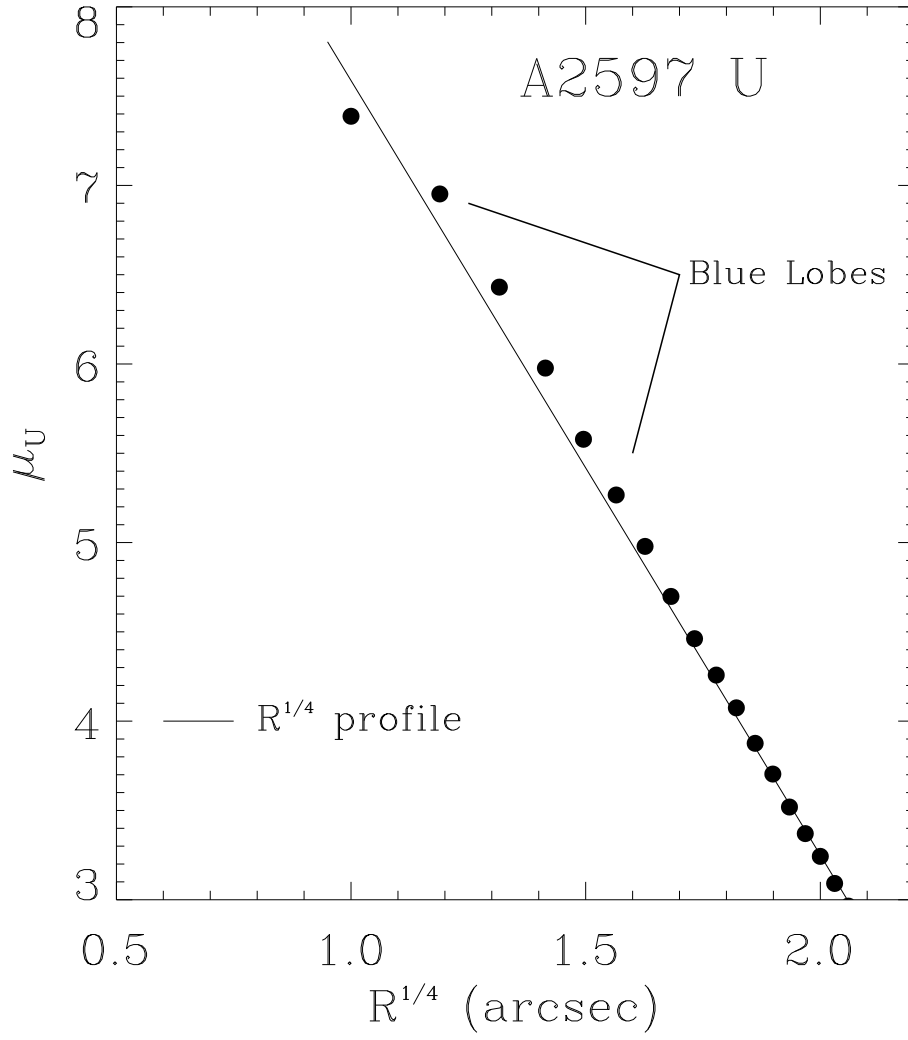


Figure 3.

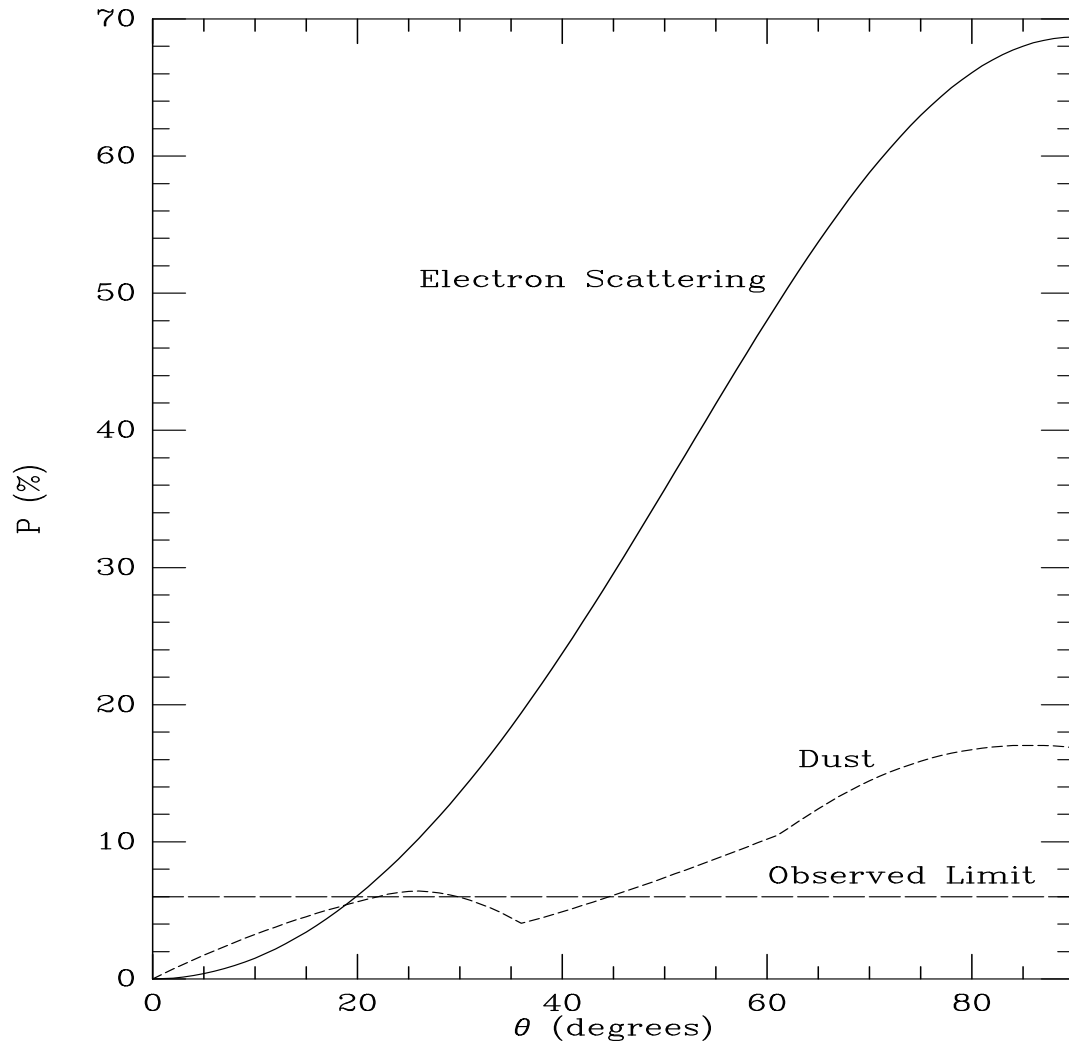


Figure 4.

